PERGAMON

International Journal of Solids and Structures 37 (2000) 7055–7069

INTERNATIONAL JOURNAL OF SOLIDS and STRUCTURES

www.elsevier.com/locate/ijsolstr

When does an adhesively bonded interfacial weak zone become the nucleus of a crack? ☆

I.V. Simonov [a,*], B.L. Karihaloo [b]

[a] *Institute of Problems of Mechanics, Russian Academy of Sciences, Moscow 117526, Russia*
[b] *School of Engineering, Cardiff University, Cardiff CF2 3TB, UK*

Received 10 November 1998

Abstract

The conditions under which an adhesively bonded weak zone (with continuously distributed adhesive forces) at the interface between two dissimilar elastic half planes can become the nucleus of a crack are derived. The problem is first reduced to a traction-free weak zone at the interface between two dissimilar elastic half planes, subjected remotely to an inhomogeneous stress field. This reduction procedure allows the general solution to be obtained in ordinary functions without the usual Cauchy integrals.

Keywords: Interface; Weak zone; Crack; Nucleus elasticity

1. Introduction

The Griffith/Irwin linear elastic fracture mechanics for ideal brittle materials is based on the model of a crack as a cut with traction-free faces. If the cut contains small zones near its tips, where cohesive forces act against the applied tensile forces and reduce their opening, then the mechanics of quasi-brittle materials is normally used (Barenblatt, 1959; Leonov and Panasyuk, 1959; Dugdale, 1960). The length of the cohesive zone, ℓ_* is much smaller than that of the crack itself, ℓ_0. There have been many recent advances in the application of the cohesive crack models to quasi-brittle materials, such as concrete, and rocks, in which the size of the cohesive zone can be commensurate with that of the crack (Hillerborg et al., 1976; Karihaloo and Nallathambi, 1990; Planas and Elices, 1992; Planas et al., 1995). A cohesive crack is one, in which a part of the crack near its centre is traction free and a part near the tips is acted upon by cohesive/adhesive forces.

The limiting situation, when the faces of the whole crack are acted upon by adhesive/cohesive forces may be regarded as a weak zone which is normally closed, but can open progressively under sufficiently large external tensile forces. It is this limiting situation, which is the topic of the present study. We are interested in establishing conditions (criteria) under which an adhesively bonded weak zone at the interface between two dissimilar elastic half planes will form the nucleus of a potential cohesive crack.

☆ This work was partly supported by INTAS Grant 96-2306 to IVS and was completed during his visit to Cardiff University.
* Corresponding author.

0020-7683/00/$ - see front matter
PII: S0020-7683(99)00324-8

The weak zone and the corresponding adhesive/cohesive forces can be of a very different physical origin – atomic, dislocational, localised porosity, entrapped dirt or air during production, etc. (see e.g. Planas et al., 1995). Healed cracks in glaciers, and in Earth's crust are also weak zones. The size of the weak zone can thus range from a few micrometres to several kilometres. Notwithstanding the size and physical origin, it is interesting to investigate the general behaviour of interfacial weak zones in much the same manner as has been done for cohesive cracks (Hillerborg et al., 1976; Planas and Elices, 1992; Planas et al., 1993; Smith, 1994; Karihaloo, 1995, 1997). For the latter, the cohesive force (in the cohesive zone), crack opening displacement relationships have been established subject to a series of physical constraints, such as the smooth closure of cohesive zone tips.

In this article, we shall consider an adhesively bonded weak zone at the interface between two dissimilar elastic half planes under a constant remote tensile stress field. Without going into the details of the physical origin of the cohesive/adhesive forces, it is assumed that they are distributed continuously over the entire extent of the zone and can be expressed in a polynomial series containing N terms. The problem is first reduced to an equivalent problem of a weak zone with traction-free faces, using the superposition method proposed by Simonov (1990). The traction-free weak zone in the equivalent problem is situated at the interface between two dissimilar elastic half planes which are now subjected remotely to an inhomogeneous stress field. The superposition method allows us to obtain the solution in ordinary functions and to avoid the usual Cauchy integrals. The general solution contains N free parameters which are fixed by imposing physically consistent constraints on the solution. In this manner, the conditions (criteria) for a pre-existing adhesively-bonded interfacial weak zone to form the nucleus of a potential cohesive crack are identified. Depending on the length of the weak zone, its transition to a percursor crack state can be stable or unstable, as well as being accompanied by a sudden release of energy.

2. Statement of the problem

Consider a weak zone, $x \in [-1, 1]$, along the interface $y = 0$ between two dissimilar elastic half planes subjected to a homogeneous tensile stress field $\sigma_\infty > 0$ at infinity (Fig. 1). Assume that the faces of the weak zone are subjected to as yet unknown adhesive/cohesive stresses which can be expanded in a series symmetrical about the x-axis

$$\sigma_c(x) = \sigma_* + \sum_{n=1}^{N} \sigma_n x^{2n}, \quad |x| < 1. \tag{1}$$

Assume further that up to $\sigma_\infty \leqslant \sigma_{th}$, where $\sigma_{th} \geqslant 0$ is the threshold stress, the faces of the weak zones are closed, i.e. the half planes are just under the applied homogeneous stress field. When the external remote tensile stress is in the range $\sigma_{th} < \sigma_\infty < \sigma_{cr}$, the faces of the weak zone move apart and a continuous adhesive/cohesive compressive force (1) acts between them to counteract the external force in such a way that the tips of the faces $(x = \pm 1)$ close smoothly. This state of the weak zone which forms the nucleus of a potential crack shall be called the precursor state. When $\sigma_\infty = \sigma_{cr}$, the adhesive force at the centre of the weak zone vanishes. The corresponding distance by which the faces have moved apart at the centre is denoted by w_{cr}. Depending on the half length of the weak zone ℓ_0 (assumed here equal to unity), different scenarios are possible until an autonomous regime for the adhesive forces is established in the near-tip zones. We shall focus our attention on the analysis of the precursor state based on general physical considerations. We mention en passant that the assumption of a smooth crack closure is normally not made in the ceramics community who allow the material ahead of the cohesive zone to be infinitely strong in tension. The real materials, including the ceramics, have a finite tensile strength consistent with the assumption made here. Moreover, it is implied that σ_{cr} is less than the interfacial tensile strength, so that it is

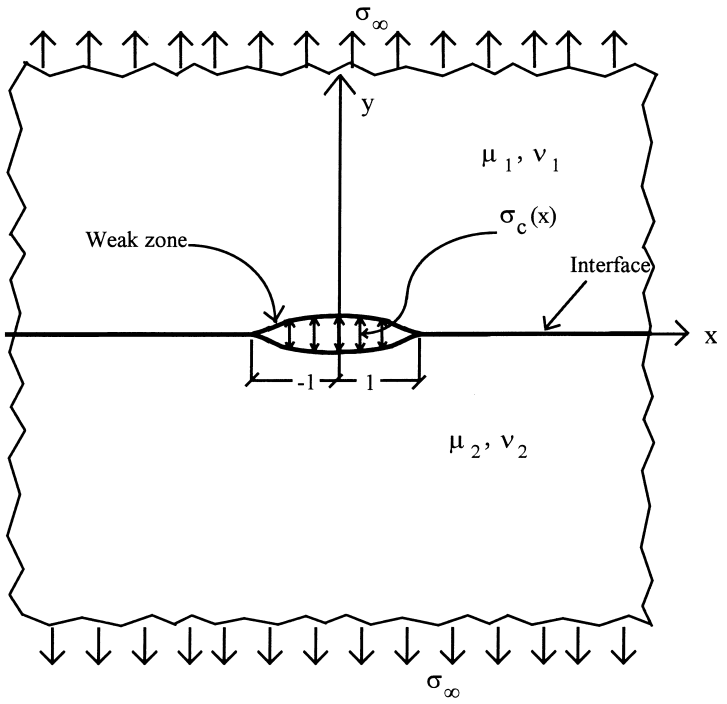

Fig. 1. A weak zone at the interface between two dissimilar isotropic half planes under a homogeneous remote tensile stress σ_∞. The weak zone is bonded by a continuous distribution of adhesive stresses $\sigma_c(x)$.

not possible for new weak zones to emerge along the interface before the weak zone under consideration opens to become a precursor crack.

The elastic fields in the two half planes can be expressed through the complex vector function $\chi = (\chi_1, \chi_2)$ (Simonov, 1985, 1990) which is related to the well-known Kolosov–Muskhelishvili complex potentials ϕ and ψ via

$$\begin{aligned} \chi_1(z) &= z\phi'(z) + \psi(z), \\ \chi_2(z) &= 2\phi(z) + \chi_1(z), \end{aligned} \tag{2}$$

where $z = x + \mathrm{i}y$, with $\mathrm{i} = \sqrt{-1}$. The complex functions χ_j $(j = 1, 2)$ are very convenient for solving plane interface problems due to their simple continuation property throughout the interface

$$\chi_j(z) = (-1)^j \overline{\chi_j(\bar{z})} \tag{3}$$

and their relationship to the stress σ_{ij} and displacement u_i fields along the interface ($y = 0$):

$$\begin{aligned} \tau &\equiv \sigma_{12} = \mathrm{Im}\,\chi_1, \\ \sigma &\equiv \sigma_{22} = \mathrm{Re}\,\chi_2, \\ u_{,x} &\equiv u_{1,x} = -\mathrm{Re}[b_j\chi_1 + a_j\chi_2], \\ v_{,x} &\equiv u_{2,x} = \mathrm{Im}[a_j\chi_1 + b_j\chi_2]. \end{aligned} \tag{4}$$

Here,

$$4\mu_j a_j = 1 - \kappa_j, \qquad 4\mu_j b_j = 1 + \kappa_j, \tag{5}$$

where μ_j are the shear moduli, $\kappa_j = 3 - 4\nu_j$ for plane strain, $\kappa_j = (3 - \nu_j)/(1 + \nu_j)$ for generalised plane stress state, and ν_j are Poisson's ratios of the two media ($j = 1,2$). The vector function χ can be continuously extended almost everywhere on the x-axis from above and below, and $y\,\mathrm{d}\chi/\mathrm{d}z \to 0$, when $y \to 0^{\pm}$.

The boundary value problem for the interface reduces to the Riemann–Hilbert problem of finding a complex vector function $\chi(z)$ which satisfies the following boundary conditions on the interface $y = 0^+$

$$\mathrm{Im}(D\chi)|_{0^+} = g(x), \tag{6}$$

where D is a piecewise constant matrix which will be defined later. At the points of discontinuity in the matrix D, say z_k, $k = 1, 2, \ldots$, and at $z \to \infty$, the vector function $\chi(z)$ behaves as

$$|\chi| < \frac{\text{const}}{|z - z_k|^{1/2}}. \tag{7}$$

When $\sigma_\infty \leqslant \sigma_{\text{th}}$, the constant stress field in the plane is given by $\chi_1^\infty = \beta\sigma_\infty$, $\chi_2^\infty = \sigma_\infty$ according to Eq. (4), where $\beta = (a_2 - a_1)/(b_1 + b_2)$ is the Dundurs mixed parameter. Without loss of generality, we will restrict our attention to $0 \leqslant \beta \leqslant 0.5$ in the sequel. Note that an interchange in the two half planes results in the reversal of the sign of β.

The boundary-value problem (6) and (7) involving inhomogeneous conditions along the interfacial weak zone is inconvenient to handle mathematically. For this reason, we shall reduce it to an equivalent problem with a traction-free interfacial weak zone subjected to an inhomogeneous stress field at infinity, using the method proposed by Simonov (1990), namely at $y = 0^+$

$$\begin{aligned} &\sigma = \tau = 0, \quad |x| < 1, \\ &[u_{,x}] = [v_{,x}] = 0, \quad |x| > 1, \\ &\int_{-1}^{1} ([u_{,x}], [v_{,x}])\,\mathrm{d}x = 0. \end{aligned} \tag{8}$$

The above homogeneous boundary conditions on the interface lead to the following homogeneous conditions in terms of the complex vector function $\chi(z)$:

$$\mathrm{Im}(D\chi)|_{0^+} = 0 \tag{9}$$

with

$$\begin{aligned} D &= \begin{pmatrix} -\beta & 1 \\ \mathrm{i} & -\mathrm{i}\beta \end{pmatrix}, \quad |x| > 1, \\ D &= \begin{pmatrix} 1 & 0 \\ 0 & \mathrm{i} \end{pmatrix}, \quad |x| < 1. \end{aligned} \tag{10}$$

The complex vector function $\chi(z)$ in Eq. (9) is, of course, further subjected to the limit conditions (7) as $z_k \to \pm 1$ (i.e. $x \to \pm 1$) and the following inhomogeneous stress field at infinity (symmetric with respect to $x = 0$):

$$\chi = \begin{pmatrix} \beta\sigma_0 \\ \sigma_0 \end{pmatrix} - \sum_{n=1}^{N} \begin{pmatrix} \beta\sigma_n \\ \sigma_n \end{pmatrix} z^{2n} + \mathrm{O}(z^{-2}), \quad z \to \infty, \tag{11}$$

where $\sigma_0 = \sigma_\infty - \sigma_* \geqslant 0$.

A general discussion of the stress field representation (11) for a piecewise elastic plane is given by Simonov (1990), but we note here that the summation term in Eq. (11) is the solution for two elastic half

planes without a weak zone along the interface. The perturbation induced by the interfacial weak zone is given by the term outside the summation sign. The stress field (11) can be decomposed into two parts

$$\chi = \chi^{\infty} - \chi^{*}, \tag{12}$$

where

$$\chi^{*} = \sigma_{*}\binom{\beta}{1} + \sum_{n=1}^{N}\binom{\beta}{1}\sigma_n z^{2n} + \mathrm{O}(z^{-2}), \quad z \to \infty, \tag{13}$$

χ^{∞} determines the field due to the external loading at infinity and χ^{*}, the perturbation due to the adhesive/cohesive stresses (1) between the faces of the interfacial weak zone. The advantage of the procedure followed above is that we shall be able to avoid Cauchy integrals and obtain the solution in terms of ordinary functions.

As mentioned in Section 1, the cohesive stresses (1) and the distance w by which the faces of the weak zone move apart, when $\sigma_{\mathrm{th}} < \sigma_{\infty} < \sigma_{\mathrm{cr}}$, have to be subjected to physically consistent additional requirements in order to determine σ_n in Eq. (1) or Eq. (13). We require $\sigma_{\mathrm{c}}(x)$ of Eq. (1) and $w(x)$ to be positive. Moreover, we require the faces of the weak zone to close smoothly near the tips to avoid stress singularities there, i.e. $w'(x)|_{x=\pm 1} = 0$. Depending upon the number of terms N in the summation (1) or Eq. (13), we may further require the curvature also to vanish near $x = \pm 1$, i.e. $w''(x)|_{x=\pm 1} = 0$. In other words,

$$\begin{aligned} &\sigma_{\mathrm{c}}(x) \geqslant 0, \quad w(x) \geqslant 0, \quad |x| < 1, \\ &w(x) \sim (1-x^2)^{3/2}, \quad |x| \to 1^{\pm}. \end{aligned} \tag{14}$$

The question arises as to whether we can justify the above requirements concerning the smooth closure, given that these would appear to contradict the expected solution for an interfacial crack which contains oscillatory singular terms near the tips. The works of Comninou and others (Comninou, 1977; Simonov, 1985, 1992) however show that the size of the overlapping zone due to oscillatory singularities is very small, less than one hundredth of the crack length, if the ratio $\sigma_{\infty}/\tau_{\infty} > 1$, where τ_{∞} is the applied shear stress at infinity. Moreover, they show that the ratio of the shear to normal displacements is

$$\frac{u}{v} \sim \frac{\tau_{\infty}}{\sigma_{\infty}} + \tan\left[\alpha \ln\left(\frac{1+x}{1-x}\right)\right], \tag{15}$$

where

$$\alpha = \frac{\ln \lambda}{2\pi}, \qquad \lambda = \frac{1+\beta}{1-\beta}. \tag{16}$$

For $0 \leqslant \beta \leqslant 0.5$, $\lambda \leqslant 3$, so that α ranges over $0 \leqslant \alpha < 0.175$. Consequently, if $\tau_{\infty} \ll \sigma_{\infty}$, the ratio (15) is very small, practically over the entire length of the weak zone, excluding negligibly small near-tip zones. Thus, the shear displacement jump, $[u_{,x}]$ in Eq. (8) can be neglected, when only the normal cohesive forces in the weak zone are considered.

3. General solution

We introduce two piecewise holomorphic functions $W_k(z)$ and write

$$\chi_j = W_1 - (-1)^j W_2. \tag{17}$$

Substitution of Eq. (17) into Eqs. (9) and (11), uncouples W_1 and W_2 which can then be written as:

$$W_1(z) = \frac{E(z)}{2\sqrt{z^2-1}}\left(\frac{1-z}{1+z}\right)^{i\alpha}, \qquad W_2(z) = \overline{W_1(\bar{z})}, \tag{18}$$

where

$$E(z) = (1-\beta^2)^{1/2}\sum_{n=0}^{2N+1} E_n z^n. \tag{19}$$

The cuts to single out branches of multi-valued functions $(1+z)^{i\alpha}, (1-z)^{i\alpha}$ and $(z^2-1)^{1/2}$ are $x \geqslant 1$ and $x \leqslant -1$, and the equalities $\arg(1-x)^{\pm} = \mp\pi$, $\arg(1+x)^{\pm} = \pm\pi$ at the upper and lower surfaces of the cuts fix these branches, so that

$$\begin{aligned} &\left[(x^2-1)^{1/2}\right]^{\pm} = \pm \operatorname{sgn} x\sqrt{x^2-1}, \quad |x| > 1, \\ &\left[(x^2-1)^{1/2}\right]^{\pm} = i\sqrt{1-x^2}, \quad |x| < 1. \end{aligned} \tag{20}$$

The coefficients E_n in Eq. (19) are determined from the inhomogeneous stress field at infinity (11), after expanding the binomials $(1 \pm z^{-1})^{i\alpha}$ and $(1-z^{-2})^{1/2}$ in Laurent series using the formula

$$(1 \pm q)^a = \sum_{k=0}^{\infty} (\pm 1)^k C_k^a q^k, \tag{21}$$

where

$$\begin{aligned} &C_0^a = 1, \\ &C_k^a = \frac{a(a-1)\cdots(a-k+1)}{k!}, \quad k > 0. \end{aligned} \tag{22}$$

The final result is

$$E_k = \sum_{j=0}^{N} \sigma_j e_j \sum (-1)^n C_n^{1/2-i\alpha} C_m^{2i\alpha}, \quad k = 0, 1, \ldots, 2N+1, \tag{23}$$

where

$$\begin{aligned} &e_j = 1, \quad j = 0, \\ &e_j = -1, \quad j \geqslant 1. \end{aligned} \tag{24}$$

The inner summation is subjected to the following restrictions:

$$\begin{aligned} &m + 2n = 1 + 2j - k, \\ &m = 0, 1, \ldots, 2N+1, \\ &n = 0, 1, \ldots, N. \end{aligned}$$

In particular, for $N=2$,

$$\begin{aligned}
E_0 &= 2\mathrm{i}\alpha\left[\sigma_0 + \frac{1+4\alpha^2}{6}\sigma_1 + \frac{1}{15}\left(\frac{11}{8} + 5\alpha^2 - 2\alpha^4\right)\sigma_2\right] \\
&= A_1\sigma_0 - (A_1B_1 + A_3B_0)\sigma_1 - (A_1B_2 + A_3B_1 + A_5B_0)\sigma_2, \\
E_1 &= \sigma_0 + (\tfrac{1}{2} + 2\alpha^2)\sigma_1 + (\tfrac{1}{8} + \tfrac{1}{3}\alpha^2 - \tfrac{2}{3}\alpha^4)\sigma_2 \\
&= \sigma_0 - (A_0B_1 - A_2B_0)\sigma_1 - (A_0B_2 + A_2B_1 + A_4B_0)\sigma_2, \\
E_2 &= 2\mathrm{i}\alpha\left[-\sigma_1 + \left(\tfrac{1}{6} + \tfrac{2}{3}\alpha^2\right)\sigma_2\right] \\
&= -A_1\sigma_1 - (A_1B_1 + A_3B_0)\sigma_2, \\
E_3 &= -\sigma_1 + \frac{1+4\alpha^2}{2}\sigma_2 \\
&= -\sigma_1 - (A_0B_1 + A_2B_0)\sigma_2, \\
E_4 &= -2\mathrm{i}\alpha\sigma_2 = -A_1\sigma_2, \\
E_5 &= -\sigma_2,
\end{aligned} \tag{25}$$

where

$$A_j = C_j^{2\mathrm{i}\alpha}, \quad B_n = C_n^{1/2-\mathrm{i}\alpha}(-1)^n. \tag{26}$$

For later use, the expression for the vertical separation of the faces of the weak zone (i.e. the vertical displacement discontinuity) is derived here

$$w(x') = \int_1^{x'} [v_{,x}]\,\mathrm{d}x = b\int_1^{x'} \mathrm{Im}\{\chi_2(x) - \beta\chi_1\}\,\mathrm{d}x, \quad |x'| < 1, \tag{27}$$

where $b = b_1 + b_2$, as

$$\chi_1 = 2\,\mathrm{Re}\,W_1, \quad \chi_2 = 2\mathrm{i}\,\mathrm{Im}W_1, \quad |x| < 1, \tag{28}$$

Eq. (27) can be written as

$$\begin{aligned}
w(x') &= 2b\int_1^{x'} \mathrm{Im}\,W_1(x)\,\mathrm{d}x \\
&= b(1-\beta^2)^{1/2}\int_{x'}^1 \frac{E_*(x)\sin f(x) + E_{**}(x)\cos f(x)}{\sqrt{1-x^2}}\mathrm{d}x,
\end{aligned} \tag{29}$$

where

$$f(x) = \ln\left(\frac{1+x}{1-x}\right)^{\alpha}, \qquad E_* = \sum_{n=0}^{N} E_{2n+1}x^{2n+1}, \qquad E_{**} = \sum_{n=0}^{N} E_{2n}x^{2n}. \tag{30}$$

3.1. Two indistinguishable half planes

We now consider the simple case when the mixed Dundurs parameter $\beta = 0$. By definition (16), α also vanishes. The situation $\beta = \alpha = 0$ covers both a homogeneous plane with a central weak zone and two dissimilar but indistinguishable half planes with an interfacial weak zone. The latter follows from the fact that $\beta = 0$ only means $a_1 = a_2$. The two half planes can still have different values of b_j. In the simple case under consideration, solution (18)–(30) is rendered symmetric about the y-axis and is considerably simplified

$$
\begin{aligned}
&\chi_1 \equiv 0, \qquad \chi_2 \equiv \chi = W_1 - W_2,\\
&W_1(z) = \frac{P(z)}{2\sqrt{z^2-1}}, \qquad W_2(z) = \overline{W_1(\bar{z})},\\
&P(z) = \sum_0^N P_n z^{2n+1},\\
&P_n = \sum_{j=0}^N \sigma_j \sum_{k=j-n} (-1)^k C_k^{1/2},\\
&\sigma_c(x) = \sigma_* + \sum_1^N \sigma_n x^{2n},\\
&w(x) = b\int_x^1 \frac{P(y)}{\sqrt{1-y^2}}\,\mathrm{d}y, \quad |x| < 1.
\end{aligned}
\tag{31}
$$

The integral in Eq. (31) is evaluated for each integer value of $n = 0, 1, \ldots, N$. Let us consider several values of N.

3.1.1. $N = 0$

In this case, Eq. (1) reduces to

$$\sigma_c(x) = \sigma_* = \text{const.} \tag{32}$$

This case is similar to the Dugdale–Leonov–Panasyuk model of a cohesive crack. The requirement that the faces of the weak zone close smoothly near the tips, demands that the principal mode I stress intensity factor K_I vanish at each tip, i.e.

$$K_I = \sum_0^N P_n = 0, \tag{33}$$

whence it follows that $P_0 \equiv \sigma_0 = 0$. The solution for this special case is therefore the trivial one

$$\sigma_0 \equiv 0, \quad \sigma_c \equiv \sigma_\infty, \quad w \equiv 0. \tag{34}$$

That is, the weak zone will never open and become the nucleus of a potential crack, irrespective of the magnitude of the remote tensile stress σ_∞. We note again that the situation would be different if the material ahead of the weak zone had infinite tensile strength so that $K_I > 0$.

3.1.2. $N = 1$

In this case, condition (33), together with the definition of P_n (31), namely $P_0 = \sigma_0 + \frac{1}{2}\sigma_1$, $P_1 = -\sigma_1$, gives $\sigma_1 = 2\sigma_0$. The corresponding cohesive force distribution over the weak zone and the relative vertical separation of its faces are

$$
\begin{aligned}
&\sigma_c = \sigma_\infty + \sigma_0(1-2t), \quad t = 1 - x^2,\\
&w(t) = \tfrac{2}{3} b\sigma_0 t^{3/2}, \quad 0 \leqslant t \leqslant 1.
\end{aligned}
\tag{35}
$$

The first of the requirements (14) leads to the inequalities

$$0 < \sigma_0 \leqslant \sigma_\infty, \quad \sigma_{th} \leqslant \sigma_\infty \leqslant \sigma_{cr} \tag{36}$$

with all other conditions being identically satisfied. Thus, the solution is a one-parameter representation of the weak zone as a percursive crack, with the free parameter σ_0 which is subjected to the conditions (36).

When $\sigma_0 \leqslant \sigma_{th}$, the solution for $N=1$ coincides with that of $N=0$ (34), as it should. When σ_∞ reaches the upper bound σ_{cr}, inequality (36) gives

$$\sigma_0 = \sigma_\infty = \sigma_{cr}. \tag{37}$$

Let us denote the maximum vertical separation of the weak zone faces (at $x=0$, i.e. $t=1$) by w_{cr} corresponding to $\sigma_0=\sigma_{cr}$ (37) and substitute it into the second of the two relations (35), and so giving

$$\sigma_{cr} = \tfrac{3}{2}\frac{w_{cr}}{b}. \tag{38}$$

This critical value of the vertical separation (assumed to be a material constant) corresponds to the onset of the formation of a crack. At this instant, the distributions (35) are completely defined through w_{cr} or σ_{cr} (Fig. 2(a))

$$\sigma_c(x) = 2\sigma_{cr}x^2, \quad w(x) = w_{cr}(1-x^2)^{3/2}. \tag{39}$$

However, when $\sigma_{th} < \sigma_\infty < \sigma_{cr}$ in (36), σ_0 cannot be expressed in terms of σ_∞. It is now necessary to measure $\sigma_0 = \sigma_\infty - \sigma_*$ experimentally, which may not be an easy task, especially if the physical source is at the microscopic level. However, we can still follow its evolution with σ_∞ in accordance with its limiting values given by (34) and (37). Let us assume $\sigma_0(\sigma_\infty)$ is a power law

$$\sigma_0(\sigma_\infty) = \sigma_{cr}\left(\frac{\sigma_\infty - \sigma_{th}}{\sigma_{cr} - \sigma_{th}}\right)^\gamma, \tag{40}$$

where

$$\begin{aligned} &\gamma > 1, \quad \sigma_{th} = 0, \\ &\gamma \geqslant 1, \quad \sigma_{th} > 0. \end{aligned} \tag{41}$$

Then the evolution of the cohesive force $\sigma_c(x)$ takes place as follows.

For $\sigma_\infty \leqslant \sigma_{th}$, $\sigma_c = \sigma_\infty = \text{const}$ (32). With an increase in σ_∞, σ_c increases gradually, reaching its maximum value $2\sigma_{cr}$ when σ_∞ reaches σ_{cr}. Thereafter, it decreases gradually to zero according to the parabolic law (39). The parabolic distribution of $\sigma_c(x)$ (35) shows that $\sigma_c(x)$ experiences a strong monotonic increase from $x=0$ to $x=1$ at each value of σ_∞ in the range $\sigma_{th} \leqslant \sigma_\infty \leqslant \sigma_{cr}$. As to $w(x)$ (35), it satisfies the requirement of smooth closure $w'(\pm 1)=0$, but at these locations the curvature is unbounded $w''(\pm 1)=\infty$. Note that elimination of x from Eq. (39) gives the constitutive law for the weak interfacial zone.

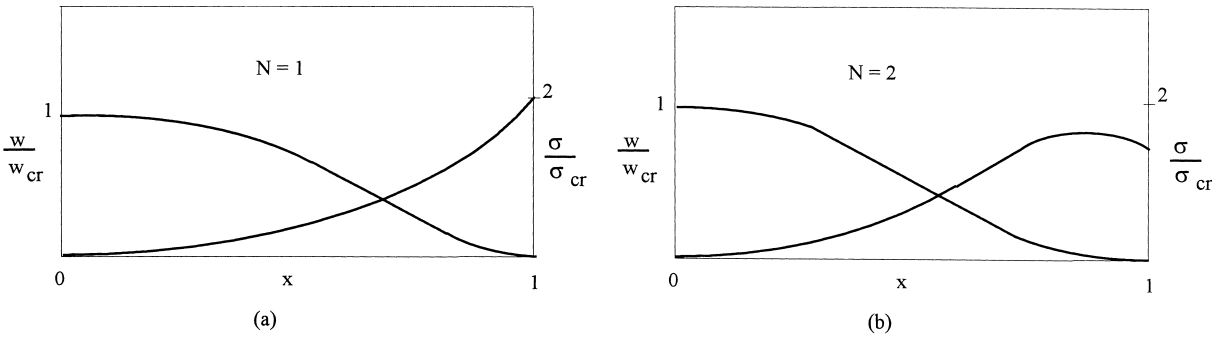

Fig. 2. The shape of the weak zone $w(x)$ under the adhesive stresses $\sigma_c(x)$ when (a) $N=1$, (b) $N=2$. The weak zone is located on the interface between two indistinguishable half planes, i.e. $\beta=\alpha=0$, but $b_1 \neq b_2$.

3.1.3. $N=2$

If we wish to impose the condition that the curvature also vanishes at the weak zone tips, then we must include an additional term in the polynomial series (1). From Eq. (31), it then follows that

$$P_0 = -\sigma_0 - \tfrac{1}{2}\sigma_1 - \tfrac{1}{8}\sigma_2, \quad P_1 = \sigma_1 - \tfrac{1}{2}\sigma_2, \quad P_2 = \sigma_2. \tag{42}$$

The conditions

$$w'(1) = 0, \quad w''(1) = 0$$

lead to

$$\sum_0^2 P_n = 0, \quad \sum_0^2 (2n+1)P_n = 0. \tag{43}$$

From Eqs. (42) and (43), it follows that

$$\sigma_1 = 4\sigma_0, \quad \sigma_2 = -\tfrac{8}{3}\sigma_0. \tag{44}$$

The corresponding distributions of $\sigma_c(x)$ and $w(x)$ (31) are

$$\begin{aligned} \sigma_c(x) &= \sigma_\infty + \sigma_0\left(4x^2 - 1 - \tfrac{8}{3}x^4\right), \\ w(x) &= \tfrac{8}{15}b\sigma_0(1-x^2)^{5/2}. \end{aligned} \tag{45}$$

The counterpart of Eq. (38) is

$$\sigma_{cr} = \frac{15}{8}\frac{w_{cr}}{b}. \tag{46}$$

We can now follow the same line of reasoning as above for $N=1$. The distributions (45) and (46) again contain just one free parameter σ_0, which may be estimated, as above (39). At the limit $\sigma_\infty = \sigma_{cr}$, both distributions are again completely defined in terms of w_{cr} (or σ_{cr} vide 46)

$$\begin{aligned} \sigma_c(x) &= 4\sigma_{cr}x^2\left(1 - \tfrac{2}{3}x^2\right), \\ w(x) &= w_{cr}(1-x^2)^{5/2}. \end{aligned} \tag{47}$$

Although the faces of the weak zone close smoothly near the tips, the distribution of the cohesive stress is no longer a monotonically decreasing function in the range $0 \leqslant |x| \leqslant 1$. It now increases with x in the range $0 < |x| < x_m = \sqrt{3}/2$, reaches its maximum value $\sigma_c(x_m) = \tfrac{3}{2}\sigma_{cr}$ at $x = x_m$, and then decreases slightly up to the value $\sigma_c = \tfrac{4}{3}\sigma_{cr}$ at $x = 1$ (Fig. 2(b)).

Again, the elimination of x from Eq. (47) gives the corresponding constitutive law relating the adhesive stress to the displacement jump.

3.2. Two dissimilar half planes

We now consider the general case when $\beta > 0,\ \alpha > 0$ in the ranges

$$0 \leqslant \beta \leqslant 0.5, \quad 0 < \alpha < 0.175. \tag{48}$$

As α^2 is small ($0 < \alpha^2 < 0.03$), we shall neglect terms of $O(\alpha^3)$ or even $O(\alpha^2)$, if the latter does not contain a factor which is large compared with unity. We again give a step-by-step analysis of the two cases $N=1$, 2. The case $N=0$ is identical to that considered above when $\beta = 0$ (Section 3.1.1). But first let us examine the

near-tip stress fields closely. Note that the sum in Eq. (23) can be expanded into real and imaginary sets of E_n as follows:

$$E_{2n} \equiv \mathrm{i}E'_{2n}, \qquad E_{2n+1} \equiv \mathrm{Re}\,E_{2n+1}, \quad n = 0, 1, \ldots, N. \tag{49}$$

In fact, this expansion was used in the derivation of coefficients (25). It is easily verified that

$$E'_{2n} = \mathrm{O}(\alpha), \quad E_{2n+1} = \mathrm{O}(1), \quad \alpha \to 0. \tag{50}$$

The functions W_j, χ_j and, consequently, the stress and strain near-tip fields possess an oscillatory singularity of the type

$$W_1 = BZ^{-1/2+\mathrm{i}\alpha}, \quad Z \to 0, \quad Z = \frac{z-1}{2}, \tag{51}$$

where

$$B = 1/4\lambda^{1/2}E(1) = \frac{1}{4}\lambda^{1/2}\sum_{n=0}^{N}(E_{2n+1} + \mathrm{i}E'_{2n}) \equiv B_1 + \mathrm{i}B_2\alpha, \quad B_1, B_2 = \mathrm{O}(1), \quad \text{as } \alpha \to 0. \tag{52}$$

In contrast to the case when $\beta = 0$ (and $\alpha = 0$), the SIF is now a complex one containing both the principal K_I and the secondary K_II components. Even when the solution of the near-tip stress fields is corrected by the method of asymptotic matching (Simonov, 1990) to account for overlapping near-tip zones of length ℓ_* so that the oscillatory singularity is replaced by a square-root one with SIF, K_II, the stress fields are

$$\begin{aligned} &K_\mathrm{II} = -\sqrt{8\pi/(1-\beta^2)}|B|, \\ &\tau \sim \frac{K_\mathrm{II}}{\sqrt{2\pi(x-1)}}, \quad \sigma \sim \frac{4\alpha|B|}{\sqrt{(1-\beta^2)\ell_*}}, \quad x \to 1^+, \\ &\sigma \sim \beta K_\mathrm{II}[2\pi(1-x)]^{1/2}, x \to 1^-, \quad |x-1| \ll \ell_* \\ &\ell_* = 4\exp\Big[-\Big(\frac{\pi}{2} + \arg B\Big)\alpha^{-1}\Big]. \end{aligned} \tag{53}$$

If we now follow the same procedure that we used in Section 3.1 to relate σ_n $(n = 1, 2, \ldots, N)$ to σ_0 and to determine the distributions $\sigma_\mathrm{c}(x)$ and $w(x)$ namely, that both B_1 (i.e. K_I) and B_2 vanish, we would violate the restrictions (14). For example, if we chose $N = 2$, we would find that $w(x)$ becomes negative well away from the tips. Moreover, this absurd feature of the solution would not disappear even when $\alpha \to 0$. This will be demonstrated below in Sections 3.2.2. We shall therefore take an alternative approach and eliminate only the principal stress intensity factor K_I (i.e. B_1). This will mean that there will be a small zone near each tip of the weak zone where the faces will overlap due to the oscillatory nature of the singularity. We will however estimate the size of these overlapping zones and show that it is negligibly small in comparison with the size of the weak zone.

3.2.1. $N = 1$

By requiring that $B_1 = 0$ (i.e. $K_\mathrm{I} = 0$) in Eq. (52), we have $E_1 + E_3 = 0$. From Eq. (25), it follows that

$$\sigma_1 = \frac{2\sigma_0}{1-4\alpha^2} \approx 2\sigma_0(1+4\alpha^2). \tag{54}$$

The expressions for E_* and E_{**} Eq. (30) then become

$$E_* \approx 2\sigma_0(1+4\alpha^2)t\sqrt{1-t}, \qquad E_{**} = 4\mathrm{i}\alpha\sigma_0(t-\tfrac{1}{3}). \tag{55}$$

The integral in Eq. (29) is now evaluated by applying the mean value theorem to the weakly variable function $\alpha \ln(1+x)$ in the range of integration, and so giving

$$w(t) \approx \tfrac{2}{3} b\sigma_0 (1-\beta^2)^{1/2}(1+4\alpha^2)[\{\cos g(t) + \tfrac{2}{3}\alpha \sin g(t)\} t^{3/2} + 2\alpha\{3\xi(t) - \sin^{-1} t^{1/2}\} t^{1/2} \sin f(t)] + \mathrm{O}(\alpha^2), \tag{56}$$

where

$$\begin{aligned} g(t) &= \alpha \ln \frac{t}{t_0}, \quad f(t) = \alpha \ln\left(\frac{1+x}{1-x}\right), \ x = \sqrt{1-t^2}, \\ \xi(t) &= \int_0^t \sqrt{\frac{y}{1-y}}\,\mathrm{d}y = \sqrt{t(1-t)} - \sin^{-1}\sqrt{t}. \end{aligned} \tag{57}$$

Note that $\xi(t) \sim t^{3/2}$, as $t \to 0^+$. t_0 results from the application of the mean value theorem to the integrated $\ln(1+x)^2$ so that $t_0 \approx 4$, $t \to 0$ and $t_0 \approx e$, $t = \mathrm{O}(1)$.

The cohesive stress distribution is given by Eq. (1)

$$\sigma_{\mathrm{c}}(x) = \sigma_* + \sigma_1 x^2 = \sigma_\infty - \sigma_0[1 - 2(1+4\alpha^2)x^2] + \mathrm{O}(\alpha^4). \tag{58}$$

The relative vertical separation of the weak zone faces is given by Eq. (56) in terms of the products of power and trigonometric functions. It should be noted that the main term in Eq. (56) is proportional to $t^{3/2} \equiv (1-x^2)^{3/2}$, as in the corresponding case of Section 3.1.2, when $\alpha = 0$. However, it is necessary to check that the roots of the equation $\cos(\alpha \ln(t/t_0)) = 0$, as well as that of $\sin(\alpha \ln(t/t_0))$ less than $t = 1$, lie as close to the tips of the weak zone as possible. The first root is less than 10^{-3} and the subsequent roots are even smaller. Thus, the oscillations of the faces are confined to negligibly small regions of the tips and for all practical purposes can be ignored.

Away from the tips (mathematically at distances $t = \mathrm{O}(1)$), $f(t) = \mathrm{O}(\alpha)$, so that sine functions are multiplied by terms of $\mathrm{O}(\alpha^2)$ without large factors and can therefore be neglected. On the contrary, $\cos g(t) = 1 + \mathrm{O}(\alpha^2)$, so that Eq. (56) reduces to

$$w(t) = \tfrac{2}{3} b\sigma_0 (1-\beta^2)^{1/2}(1+4\alpha^2) t^{3/2} + \mathrm{O}(\alpha^2), \tag{59}$$

which is the same as for the case of $\beta = \alpha = 0$ in Section 3.1.2 (35), apart from the factor $\sqrt{1-\beta^2}$ and the small term $(1+4\alpha^2)$. Thus, the conclusions of Section 3.1.2 remain in force. In particular, the distributions of $\sigma_{\mathrm{c}}(x)$ and $w(x)$ would be identical to that shown in Fig. 2(a), but with a different vertical scale for $\sigma_{\mathrm{c}}(x)$. It would be multiplied by the small term $(1+4\alpha^2)$, and the critical stress σ_{cr} would be

$$\sigma_{\mathrm{cr}} = \frac{3}{2}\frac{w_{\mathrm{cr}}}{b}(1-\beta^2)^{-1/2}(1+4\alpha^2)^{-1}. \tag{60}$$

3.2.2. $N = 2$

By requiring $B_1 = 0$ (i.e. $K_{\mathrm{I}} = 0$) in Eq. (52), we have $E_1 + E_3 + E_5 = 0$. From Eq. (25), it follows that

$$\sigma_1 = (2+8\alpha^2)\sigma_0 - (\tfrac{3}{4} - \tfrac{5}{8}\alpha^2)\sigma_2 + \mathrm{O}(\alpha^4). \tag{61}$$

The expressions for E_* and E_{**} (30) after the elimination of σ_1 become

$$\begin{aligned} E_* &= xt[(2+8\alpha^2)\sigma_0 + \tfrac{3}{4}(1 - \tfrac{4}{9}\alpha^2)\sigma_2 - \sigma_2 t] + \mathrm{O}(\alpha^4), \\ E_{**} &= 2\mathrm{i}\alpha[-\tfrac{2}{3}\sigma_0 - \tfrac{7}{60}\sigma_2 + (2\sigma_0 + \tfrac{13}{12}\sigma_2)t - \sigma_2 t^2] + \mathrm{O}(\alpha^3). \end{aligned} \tag{62}$$

The integrals in Eq. (29) are again evaluated using the mean value theorem to give

$$\int_x^1 E_* t^{-1/2} \cos f(x)\,\mathrm{d}x \approx t^{3/2}\Big[\Big(\frac{c_1}{3}-\frac{\sigma_2}{5}t\Big)\cos g(t) + 2\alpha\Big(\frac{c_1}{9}-\frac{\sigma_2}{25}\Big)\sin g(t)\Big], \tag{63}$$

$$\int_x^1 E_{**} t^{-1/2} \sin f(x)\,\mathrm{d}x \approx 2\alpha\big[c_2 \sin^{-1} t^{1/2} + c_3\xi(t) - \sigma_2\zeta(t)\big]\sin f(t), \tag{64}$$

where $g(t)$, $f(t)$ and $\xi(t)$ are defined in Eq. (57), and

$$\begin{aligned} \zeta(t) &= \int_0^t \sqrt{\frac{y^3}{1-y}}\,\mathrm{d}y, \\ c_1 &= (2+8\alpha^2)\sigma_0 + \tfrac{3}{4}\big(1-\tfrac{4}{9}\alpha^2\big)\sigma_2, \\ c_2 &= -\tfrac{2}{3}\sigma_0 - \tfrac{7}{60}\sigma_2, \quad c_3 = 2\sigma_0 + \tfrac{13}{12}\sigma_2. \end{aligned} \tag{65}$$

Note that $\zeta(t) \sim t^{5/2},\ t \to 0^+$. The vertical separation of the faces of the weak zone can now be written as:

$$\begin{aligned} w(t) = b(1-\beta^2)^{1/2}\Big[t^{3/2}\Big\{\Big(\frac{c_1}{3}-\frac{\sigma_2}{5}t\Big)\cos g(t) + 2\alpha\Big(\frac{c_1}{9}-\frac{\sigma_2}{25}\Big)\sin g(t)\Big\} \\ + 2\alpha\Big\{c_2 \sin^{-1} t^{1/2} + c_3\xi(t) - \sigma_2\zeta(t)\Big\}\sin f(t)\Big] + \mathrm{O}(\alpha^2). \end{aligned} \tag{66}$$

As in the case of $N=2$, $\beta=0$ (Section 3.1.3), the expression for $w(t)$ contains terms of different orders in t. This has implications for the solution as $t \to 0$. Note first the existence of the singular term $\sin^{-1}\ t^{1/2}$, $t \to 0$, but as it is multiplied by a factor $\mathrm{O}(\alpha)$, it disappears as $\alpha \to 0$. For finite α, the singular term makes a significant contribution in a very small region near $t=0$ $(x=1)$, where the contribution of the term $f(t) = \alpha \ln(1 + x^2/t)$ is pronounced, i.e. in the region $0 < t \leqslant 10^{-3}$. When $t > \varepsilon \sim 10^{-2}$, the function $\alpha \sin f(t)$ is of the order $\mathrm{O}(\alpha^2)$, and can therefore be neglected.

On the contrary, if one tried to suppress the singularity, as mentioned above, by imposing the condition $B_2 = 0$ (i.e. $K_{\mathrm{II}} = 0$), it would mean that c_2 would have to be equated to zero. Then from Eqs. (65) and (61), σ_2 and σ_1 could be expressed via σ_0 as follows:

$$\sigma_2 \approx -\tfrac{40}{7}\sigma_0, \quad \sigma_1 \approx \big(\tfrac{44}{7} - \tfrac{32}{21}\alpha^2\big)\sigma_0. \tag{67}$$

The main (first) term in formula (66) for $w(x)$ would now be multiplied by the factor $(x^2 - \frac{1}{3} - \frac{26}{9}\alpha^2)$. Bearing in mind, the range of variation of α (48), the term $\frac{26}{9}\alpha^2$ would range over $0 \leqslant \frac{26}{9}\alpha^2 < 0.087$, whence it follows that at $x = x_* \in]0,1]\,(x_* \approx \sqrt{3}/3 \approx 0.57)$, the vertical separation $w(x)$ of the faces of the weak zone would change sign, thus violating the condition $w(x) \geqslant 0,\ |x| \leqslant 1$ far from the tips. It was for this reason that we adopted the alternative approach and allowed the faces to wrinkle in very small near-tip regions $0 < t < 10^{-3}$, as shown above. In these regions, the microstructure of the material begins to play a significant role.

We have demonstrated above that most terms in Eq. (65) are of the order $\mathrm{O}(\alpha^2)$ in the range $\varepsilon < t \leqslant 1$ $(\varepsilon \sim 10^{-2})$, including the term $\cos g(t) \approx 1 + \mathrm{O}(\alpha^2)$. Expression (66) can therefore be written as

$$w(t) = \frac{b}{3}(1-\beta^2)^{1/2} t^{3/2}\big(c_1 - \tfrac{3}{5}\sigma_2 t\big) + \mathrm{O}(\alpha^2), \quad 0 < \varepsilon < t < 1. \tag{68}$$

The corresponding cohesive force distribution over the percursive crack is

$$\sigma_{\mathrm{c}}(x) = \sigma_* + \sigma_1 x^2 + \sigma_2 x^4. \tag{69}$$

By requiring that $w(t) > 0,\ \varepsilon < t \leqslant 1$, and $\sigma_{\mathrm{c}}(x) > 0,\ 0 < x \leqslant 1$, and by assuming $\sigma_2 = -d\sigma_0$, we can solve the inequalities $w(t) > 0$ and $\sigma_{\mathrm{c}}(x) > 0$ and obtain

$$0 < d \leqslant \tfrac{8}{3}\left(1 + \tfrac{40}{9}\alpha^2\right) + \mathrm{O}(\alpha^4). \tag{70}$$

At the upper limit of $d = \frac{8}{3}(1 + \frac{40}{9}\alpha^2) + \mathrm{O}(\alpha^4)$, the coefficient c_1 in Eq. (68) vanishes, as can be confirmed from Eq. (65). Thus, the expression for $w(t)$ reduces to

$$w(t) = \tfrac{8}{15}b(1-\beta^2)^{1/2}\left(1 + \tfrac{40}{9}\alpha^2\right)\sigma_0 t^{5/2} + \mathrm{O}(\alpha^2), \tag{71}$$

where we have retained the term of $\mathrm{O}(\alpha^2)$ in the parenthesis because it is multiplied by a large factor.

When β, $\alpha \to 0$, expression (71) coincides with the case $\beta = 0$, $N = 2$ studied in Section 3.1.2 (see expression (45)).

The cohesive force distribution corresponding to Eq. (71) is

$$\sigma_c(x) = \sigma_* + \tfrac{8}{3}\sigma_0\left(1 + \tfrac{40}{9}\alpha^2\right)x^2\left(\tfrac{3}{2} - 2\alpha^2 - x\right) + \mathrm{O}(\alpha^4). \tag{72}$$

As before, both distributions (71) and (72) depend on one free parameter σ_0, $0 \leqslant \sigma_0 \leqslant \sigma_{cr}$, which can be defined in terms of σ_{cr} (or w_{cr}) at the instant of the formation of a crack from the adhesively-bonded weak zone when $\sigma_0 = \sigma_\infty = \sigma_{cr}$, where

$$\sigma_{cr} = (1-\beta^2)^{-1/2}\left(1 + \tfrac{40}{9}\alpha^2\right)^{-1}\frac{15 w_{cr}}{8b}. \tag{73}$$

As in Section 3.1.2, $\sigma_c(x)$ according to Eq. (72) does not vary monotonically. It increases first from σ_* up to its maximum value $\sigma_c(x_m) \approx \sigma_* + \frac{3}{2}\sigma_0(1 + \frac{16}{9}\alpha^2)$, where $x_m^2 = \frac{3}{4} - \alpha^2 (x_m \approx 0.86)$, and then decreases reaching the value $\sigma_c(1) \approx \sigma_* + \frac{3}{4}\sigma_0(1 + \frac{4}{9}\alpha^2)$ at the tip of the weak zone. Again, the distribution of $\sigma_c(x)$ and $w(x)$ would be similar to those shown in Fig. 2(b), apart from a slight change in the vertical scale of $\sigma_c(x)$ and the definition of σ_{cr} which now includes β and α (73), besides w_{cr} and b.

4. Discussion and conclusions

The conditions under which an adhesively bonded weak zone along the interface of two dissimilar elastic half planes can become the nucleus of a potential crack are analysed. Without specifying the physical origin of the adhesive forces other than assuming that they can be expressed in a power series, the conditions under which an initially closed interfacial weak zone will open to the extent that the adhesive forces can no longer counteract the remotely applied tensile force are examined. It is found that, when the adhesive force is continuously, but non-uniformly distributed over the weak zone, the latter will become the nucleus of a potential crack when the applied tensile stress σ_∞ reaches the limiting value σ_{cr}. σ_{cr} is related to the maximum separation w_{cr} that the faces of the weak zone can tolerate before they begin to lose their adhesive strength and the Dundurs parameters α, β. The criterion for the transformation of an adhesively bonded interfacial weak zone into a crack under a remotely applied tensile stress σ_∞ may therefore be written as:

$$\sigma_\infty = A(\sigma_c(x), \ell_0, \beta) w_{cr}, \tag{74}$$

where A is a dimensioned function, determined by the distribution of the adhesive forces over the weak zone, its length and the elastic mismatch parameter. This criterion for the transition from the precursor state to a crack plays the same role as the Griffith/Irwin criterion for the growth of a traction-free crack.

The transformation of a weak zone into a crack breaks the continuity of the medium which can have highly undesirable consequences. For example, highly pure superstrength materials can suddenly lose strength. Composite superconductors, in which such a transformation would be accompanied by irreversible thermal processes, would lose superconductivity. Healed cracks (i.e. weak zones) in glaciers and Earth's crust could lead to sudden and catastrophic release of energy.

References

Barenblatt, G.I., 1959. On equilibrium cracks forming during brittle fracture. Prikladnaya Matematika i Mekhanika (PMM) 23, 434–444 (in Russian).

Comninou, M., 1977. The interface crack. ASME Journal of Applied Mechanics 44, 631–636.

Dugdale, D.S., 1960. Yielding of steel sheets containing slits. Journal of Mechanics and Physics of Solids 8, 100–104.

Hillerborg, A., Modéer, M., Petersson, P.E., 1976. Analysis of crack formation and growth in concrete by means of fracture mechanics and finite elements. Cement and Concrete Research 6, 773–782.

Karihaloo, B.L., 1995. Fracture Mechanics and Structural Concrete. Addison Wesley, Longman, UK, pp. 330 + xiv.

Karihaloo, B.L., 1997. Scaling effects in the fracture of quasi-brittle materials and structures. In: Willis, J.R. (Ed.), Proc IUTAM Symposium on Nonlinear Analysis of Fracture, Kluwer Academic, Dordrecht, pp. 13–22.

Karihaloo, B.L., Nallathambi, P., 1990. Effective crack model for the determination of fracture toughness of concrete. Engineering Fracture Mechanics 35, 637–645.

Leonov, M.Ya., Panasyuk, V.V., 1959. Growth of the minutest cracks in a brittle body. Prikladnaya Mekhanika (PM) 5, 391–401 (in Russian).

Planas, J., Elices, M., 1992. Asymptotic analysis of a cohesive crack: 1. Theoretical background. International Journal of Fracture 55, 153–177.

Planas, J., Elices, M., Gonzalo, R., 1993. The equivalent elastic crack: 2. X–Y equivalences and asymptotic analysis. International Journal of Fracture 61, 231–246.

Planas, J., Elices, M., Guinea, G.V., 1995. The extended cohesive crack. In: Baker, G., Karihaloo, B.L. (Eds.), Fracture of Brittle Disordered Materials: Concrete, Rock and Ceramics. Spons, London, 51–65.

Simonov, I.V., 1985. Interface crack in a homogeneous stress field. Mechanics of Composite Materials (MCS) 6, 969–976 (in Russian).

Simonov, I.V., 1990. An interface crack in an inhomogeneous stress field. International Journal of Fracture 46, 223–235.

Simonov, I.V., 1992. Prediction of arbitrary crack growth from the interface between dissimilar elastic materials. International Journal of Fracture 57, 349–363.

Smith, E., 1994. The elastically equivalent softening zone size for an elastic-softening material I. Power law softening behaviour, II. A simple piecewise softening law. Mechanics of Materials 17, 363–378.